AIMS Mathematics, 10(3): 4915–4937.
DOI: 10.3934/math.2025225
Received: 23 December 2024
Revised: 02 February 2025
Accepted: 17 February 2025
Published: 06 March 2025

https://www.aimspress.com/journal/Math

Research article

Symmetry, Hopf bifurcation, and offset boosting in a novel chameleon system

Jie Liu[1], Bo Sang[1,*], Lihua Fan[1], Chun Wang[1], Xueqing Liu[1], Ning Wang[2] and Irfan Ahmad[3]

[1] School of Mathematical Sciences, Liaocheng University, Liaocheng 252059, Shandong, China
[2] School of Microelectronics and Control Engineering, Changzhou University, Changzhou 213159, Jiangsu, China
[3] Faculty of Science and Engineering, Maynooth International Engineering College, Maynooth University, Maynooth, Co. Kildare W23, Ireland

* **Correspondence:** Email: sangbo_76@163.com.

Abstract: Chameleon systems are dynamical systems that exhibit either self-excited or hidden oscillations depending on the parameter values. This paper presents a comprehensive investigation of a quadratic chameleon system, including an analysis of its symmetry, dissipation, local stability, Hopf bifurcation, and various chaotic dynamics as the control parameters (μ, a, c) vary. Here, μ serves as the dissipation parameter in the y direction. Bifurcation analysis for four scenarios with $\mu = 0$ was performed, revealing the emergence of various dynamical phenomena under different parameter settings. Offset boosting means introducing a constant into one of the state variables of the system for boosting the variable to a different level. Additionally, hidden chaotic bistability with offset boosting was exhibited by varying μ. The parameter μ serves as both the Hopf bifurcation parameter and the offset boosting parameter, while the other parameters (a, c) also play critical roles as control parameters, resulting in period-doubling routes to self-excited or hidden chaotic attractors. These findings enrich our understanding of nonlinear dynamics in quadratic chameleon systems.

Keywords: Hopf bifurcation; antimonotonicity; bifurcation diagram; hidden chaotic attractor; offset boosting
Mathematics Subject Classification: 37D45, 37G35

1. Introduction

Chaos theory is a field of study that involves the mathematical analysis of complex deterministic systems exhibiting unstable aperiodic behavior. In chaotic systems, even a tiny difference in the initial conditions can lead to significantly different outcomes over time. As a way of understanding and

describing the long-term behavior of a chaotic system, a chaotic attractor has at least one positive Lyapunov exponent [1]. Bifurcation diagrams can provide insights into the mechanisms behind the chaotic behavior. After transients decay, bifurcation diagrams can be constructed by recording either the Poincaré section intersections or the local peaks of the system's trajectory. By understanding the underlying mechanisms, it is possible to control and predict the behavior of the system. Amplitude control refers to the ability to regulate the magnitude of a signal, typically in the context of chaotic systems. It was shown in [2] that symmetric chaotic systems can be both multistable and also have an independent amplitude control parameter. Chaos has found applications across various fields, including economics [3], cryptography [4], and robotics [5], among others.

In their work on Chua circuits, Leonov, Kuznetsov et al. [6–8] introduced the classification of attractors as hidden or self-excited, and they proposed an effective procedure for localizing hidden attractors based on homotopy and numerical continuation. The classification is a crucial concept, which represents a contemporary extension of Andronov's theory of oscillations and provides a fundamental understanding of the existence and characteristics of hidden oscillatory behavior in chaotic models [9, 10].

A self-excited attractor refers to an attractor whose basin of attraction intersects an open neighborhood of an equilibrium. It can be numerically found by plotting the trajectory of the system with random initial conditions near the equilibria. On the other hand, a hidden attractor is an attractor whose basin of attraction does not intersect with small neighborhoods of any equilibrium points. This implies that it cannot be numerically found using random initial conditions and demands special analytical-numerical procedures to locate its basin of attraction. In practice, there is a need to control the hidden attractors, because some structures (such as bridges or airplane wings) can display catastrophic responses under disturbances [11, 12]. According to [13], a saddle focus of index 2 is defined by an equilibrium with three eigenvalues: one real γ and a pair of complex conjugates $\sigma \pm j\omega$, where $\gamma < 0$ and $\sigma > 0$. Shilnikov homoclinic and heteroclinic theorems provide sufficient conditions for the existence of self-excited chaotic attractors in 3D systems with unstable hyperbolic equilibria. Saddle-foci with an index of 2 are frequently encountered in such systems. As noted by Zhou and Chen [14], the chaotic attractors of Lorenz, Rössler, Chua, Chen, and many other systems are in the sense of Shilnikov, but not all chaotic attractors are of Shilnikov sense. Beyond the scope of Shilnikov theorems, many chaotic flows with various types of non-hyperbolic equilibria were introduced [15–17]. Li and Hai [18] introduced a three-dimensional robust chaotic system with two non-hyperbolic equilibrium points, exhibiting features of amplitude and position modulation. It is shown that the presence of linear terms is not essential in producing complex behaviors [19].

In a review paper, Jafari et al. [20] noted that dissipative hidden chaotic flows can be categorized into three types: those with a stable equilibrium [21, 22], those without equilibrium [23], and those with an infinite number of equilibria [24]. Molaie et al. [25] proposed twenty-three chaotic flows with a single stable equilibrium point. Jafari and Sprott [26] proposed nine chaotic flows with hidden attractors that have a line equilibrium. Kumarasamy et al. [27] investigated how saddle-node bifurcations contribute to the emergence of hidden attractors, both in systems with stable equilibrium points and those without equilibrium points. Antimonotonicity refers to the intertwined creation and destruction of periodic orbits in nonlinear dynamical systems, leading to inevitable reversals of bifurcation cascades [28]. For a family of jerk systems with a hyperbolic tangent function, Li et al. [29] illustrated that antimonotonicity is important in elucidating the generation mechanism of

hidden attractors with a stable equilibrium. Recently, Dong et al. [30] investigated a chaotic system that has no equilibrium through numerical simulations and circuit implementations, and discussed engineering applications such as synchronization, offset boosting control, and image encryption.

A chameleon system is a chaotic system that, as parameter values vary, can exhibit various types of chaotic attractors, including self-excited attractors and the three types of hidden attractors. This feature provides flexibility in applications needing different types of chaotic signals. In a review paper, Sprott [31] categorized chaotic flows from a quadratic family based on equilibrium points, in which both self-excited and hidden attractors are involved. Jafari et al. [32] introduced a chameleon system with quadratic nonlinearities, contributing to an enhanced understanding of chaotic attractors, especially those that are hidden. Recall that a hyperchaotic system is defined as a dynamical system that exhibits chaotic behavior, characterized by the presence of multiple positive Lyapunov exponents. Motivated by [32], Rajagopal et al. [33] presented a hyperchaotic chameleon system, contributing to a deeper understanding of hidden chaotic flows of higher dimensions. Natiq et al. [34] presented a chameleon system with a trigonometric nonlinear controller. Cang et al. [35] investigated the hidden and self-excited coexisting attractors in the Yang system [36]. Signing et al. [37] introduced a chameleon cryptosystem that combines chameleon chaotic systems with dynamic DNA coding to enhance image encryption security through the use of chaotic sequences. Fan et al. [38] investigated the two-parameter space bifurcation of the Wei chameleon system. Recently, Tiwari et al. [39] introduced a class of quadratic chameleon systems that allow for the coexistence of hidden chaotic attractors and conservative tori.

A Hopf bifurcation is a local bifurcation where an equilibrium of a dynamical system changes stability as a parameter is varied. This phenomenon occurs when the equilibrium possesses a pair of purely imaginary eigenvalues, accompanied by specific transversality conditions and an absence of zero eigenvalues. The bifurcation can be classified as either supercritical or subcritical, resulting in either a stable or an unstable limit cycle within an invariant two-dimensional manifold, respectively. The latter situation presents a potential risk, as stable, large-amplitude limit cycles can coexist with the stable equilibrium point [40]. Stankevich et al. [41] and Zhao et al. [42] studied the dynamics of the Chua systems, establishing a connection between subcritical Hopf bifurcations of equilibria and the emergence of hidden attractors. Using a family of quadratic jerk systems, Liu et al. [43] also showed that subcritical Hopf bifurcations are closely related to the emergence of hidden attractors. Yang et al. [44] proposed a 7D hyperchaotic system with five positive exponents and investigated Hopf bifurcation to understand how complex dynamics emerge in this system. Li and Chen [45] demonstrated the complex neuromorphic behaviors of a novel current-controlled Chua corsage memristor-based neuron circuit through Hopf bifurcation and edge-of-chaos analysis. Liu et al. [46] explored a 4D hyperchaotic system through Hopf bifurcation analysis and the linear control method.

The design of a chaotic system with independent non-bifurcation parameters faces a significant challenge due to the broadband random-like nature of chaos [47, 48]. Signal polarity refers to whether a signal oscillates around zero (bipolar) or around a non-zero reference level (unipolar). Offset boosting involves adjusting the average value of a state variable by introducing a constant term into the system model, resulting in signal offset and enabling control of signal polarity. Li et al. [49] proposed an offset boosting-based strategy for the identification of multistability in dynamical systems, employing nonbifurcation operations for diagnosing multistability. In chaotic and hyperchaotic systems [50, 51], offset boosting controls have been implemented, enabling direct offset regulation through the use of a

single constant.

The paper is organized as follows. In Section 2, we introduce a novel chameleon system and conduct a detailed study on its symmetry, dissipation, stability analysis, Hopf bifurcation, and chaotic dynamics with μ varying. In Section 3, we perform a bifurcation analysis for scenarios 1 to 4 with $\mu = 0$. We investigate the system's behavior under various parameter values, focusing on the emergence of different dynamical phenomena. In Section 4, we investigate hidden chaotic bistability with offset boosting through the variation of μ. In the final section, we synthesize our key findings and discuss their implications.

2. A new chameleon system

Consider the quadratic system

$$\begin{cases} \dfrac{dx}{dt} = y, \\ \dfrac{dy}{dt} = -x + y(z + \mu), \\ \dfrac{dz}{dt} = f(x, y, z), \end{cases} \tag{2.1}$$

where

$$f(x, y, z) = a - b\,z + c\,y^2 - 0.7\,x^2 - 3\,xy.$$

It is symmetric with respect to 180-degree rotation about the z-axis. This means that the system is invariant with respect to the transformation $(x, y, z) \to (-x, -y, z)$, corresponding to a 180-degree rotation about the z-axis.

Let $h = (h_1, h_2, h_3)$ be the vector field of system (2.1). Thus the divergence function is

$$\nabla \cdot V = h_{1x} + h_{2y} + h_{3z} = -b + (z + \mu).$$

It is clear that system (2.1) is not always dissipative as the divergence depends on z. However, in specific regions of the phase space where the condition $\nabla \cdot V < 0$ holds on average, we have a dissipative flow. Due to the symmetry, system (2.1) can have a symmetrical attractor or a symmetric pair of coexisting attractors.

2.1. Stability analysis

If $a = b = 0$, system (2.1) has a line equilibrium along the z-axis. This means that every point $(0, 0, z_0)$ on the axis is an equilibrium point.

If $a \neq 0$ and $b = 0$, we have $f(0, 0, z) = a \neq 0$. Hence, there is no equilibrium point. When $x = y = 0$, we have $\dfrac{dx}{dt} = \dfrac{dy}{dt} = 0$ and $\dfrac{dz}{dt} = a \neq 0$. This indicates that the z-axis is invariant under the system's flow. The direction of the flow along the z-axis is determined by the sign of a: if $a > 0$, the flow is in the forward direction; if $a < 0$, the flow is in the backward direction.

If $b \neq 0$, there exists a unique equilibrium $P : (0, 0, a/b)$. The Jacobian matrix of system (2.1) at P is

$$A = \begin{bmatrix} 0 & 1 & 0 \\ -1 & \mu + \dfrac{a}{b} & 0 \\ 0 & 0 & -b \end{bmatrix}.$$

The corresponding characteristic polynomial is

$$\begin{aligned}\varphi_A(\lambda) &= \lambda^3 + p_1\,\lambda^2 + p_2\,\lambda + p_3\\ &= (\lambda + b)\Big(\lambda^2 - (\mu + \frac{a}{b})\,\lambda + 1\Big).\end{aligned} \tag{2.2}$$

Proposition 2.1. *Consider system* (2.1) *with* $b \neq 0$*. It is locally asymptotically stable around P if*

$$b > 0 \text{ and } a < -b\mu. \tag{2.3}$$

Proof. From (2.2) and Routh-Hurwitz criterion, the equilibrium P of system (2.1) is asymptotically stable if $b > 0$ and $\mu + \frac{a}{b} < 0$. Such constraints are equivalent to the inequalities stated in (2.3). Thus the conclusion holds. □

Corollary 2.1. *Consider system* (2.1) *with* $b > 0$ *and* $a < -b\mu$*, and let*

$$\Delta = \left(\mu + \frac{a}{b}\right)^2 - 4.$$

We have the following conclusions.

(i) If $\Delta < 0$*, then the equilibrium P is a stable node-focus.*
(ii) If $\Delta \geq 0$*, then the equilibrium P is a stable node.*

Proof. (i) Assume that $\Delta < 0$. From (2.2), we know that the characteristic polynomial has a negative root and a pair of complex conjugate roots with a negative real part. Thus the equilibrium P is a stable node-focus.

(ii) Assume that $\Delta \geq 0$. From (2.2), we know that the characteristic polynomial has three negative roots, counted with multiplicity. Therefore, the equilibrium P is a stable node. □

Assume $a, b \neq 0$ and $\mu = 0$. Then system (2.1) can assume all types of hyperbolic equilibrium points at $P:\ (0, 0, a/b)$.

Corollary 2.2. *Consider system* (2.1) *with* $b \neq 0$ *and* $\mu = 0$*. The following statements hold.*

(i) It is locally asymptotically stable around P if $a < 0$ *and* $b > 0$*. In this case, if* $a > -2b$*, then the equilibrium P is a stable node-focus; if* $a \leq -2b$*, then the equilibrium is a stable node.*
(ii) If $a > 0$ *and* $b > 0$*, the equilibrium P is unstable. In this case, if* $a < 2b$*, the equilibrium P is a saddle-focus of index 2; if* $a \geq 2b$*, the equilibrium P is a saddle of index 2.*
(iii) If $b < 0$*, the equilibrium P is unstable. In this case, if* $0 < a < -2b$*, the equilibrium P is a saddle-focus of index 1; if* $a \geq -2b$*, the equilibrium P is a saddle of index 1; if* $2b < a < 0$*, the equilibrium P is an unstable node-focus; and if* $a \leq 2b$*, the equilibrium P is an unstable node.*

Proof. (i) By setting $\mu = 0$, the statements follow from Proposition 2.1 and Corollary 2.1.

(ii) Setting $\mu = 0$, then the characteristic polynomial (2.2) becomes

$$\varphi_A(\lambda) = (\lambda + b)(\lambda^2 - \frac{a}{b}\lambda + 1). \tag{2.4}$$

Since $a > 0$ and $b > 0$, the quadratic factor of (2.4) can have a root with a positive real part. Thus the equilibrium P is unstable.

Assume that $a, b > 0$. If $a < 2b$, the cubic polynomial (2.4) has a negative root and a pair of complex conjugate roots with a positive real part. Therefore, the equilibrium P is a saddle-focus of index 2. If $a \geq 2b$, the cubic polynomial (2.4) has a negative root and two positive roots. Therefore, the equilibrium P is a saddle of index 2.

(iii) If $b < 0$, the characteristic polynomial (2.4) has a positive root $\lambda = -b$. Thus the equilibrium P is unstable. The rest of the proof for classifying the equilibrium is similar to that of case (ii). □

2.2. Hopf bifurcation with μ varying

When $a = 0$, system (2.1) becomes

$$\begin{cases} \dfrac{dx}{dt} = y, \\ \dfrac{dy}{dt} = -x + y(z + \mu), \\ \dfrac{dz}{dt} = -b\,z + c\,y^2 - 0.7\,x^2 - 3\,xy. \end{cases} \tag{2.5}$$

It has a unique equilibrium point at the origin. Here we assume that $b > 0$.

Proposition 2.2. *When $\mu = 0$, a Hopf bifurcation occurs at the origin for system* (2.5).

Proof. The characteristic polynomial of this system is

$$\varphi_A(\lambda) = \lambda^3 + p_1(\mu)\,\lambda^2 + p_2(\mu)\,\lambda + p_3(\mu),$$

where

$$p_1 = -\mu + b,\ p_2 = -b\,\mu + 1,\ p_3 = b.$$

Note that

$$(p_1 p_2 - p_3)(\mu) = b\,\mu^2 - \left(1 + b^2\right)\mu.$$

So

$$(p_1 p_2 - p_3)(0) = 0, \tag{2.6}$$

$$(p_1 p_2 - p_3)'(0) = -(1 + b^2) < 0. \tag{2.7}$$

Thus, a Hopf bifurcation occurs from the origin at $\mu = 0$. □

When $\mu = 0$, system (2.5) becomes

$$\begin{cases} \dfrac{dx}{dt} = y, \\ \dfrac{dy}{dt} = -x + F^2, \\ \dfrac{dz}{dt} = -b\,z + F^3, \end{cases} \tag{2.8}$$

where

$$F^2 = yz,$$

$$F^3 = c\,y^2 - 0.7\,x^2 - 3\,xy.$$

According to [52], the first Lyapunov number a_1 at the Hopf bifurcation can be obtained as

$$a_1 = \frac{-2}{16\,\lambda_3} F^2_{yz}\left(F^3_{xx} + F^3_{yy}\right) + \frac{F^2_{yz}}{16\,(4\omega^2 + \lambda_3^2)}\left(\lambda_3\left(F^3_{xx} - F^3_{yy}\right) + 4\omega F^3_{xy}\right), \tag{2.9}$$

where $\lambda_3 = -b$ and $\omega = -1$.

By a simple computation, we have

$$a_1 = \frac{(30c - 7)\,b^2 + 60b + (80c - 56)}{80b\,(b^2 + 4)}. \tag{2.10}$$

Let us consider the following system:

$$\begin{cases} \dfrac{dx}{dt} = y, \\ \dfrac{dy}{dt} = -x + y(z + \mu), \\ \dfrac{dz}{dt} = -b\,z + y^2 - 0.7\,x^2 - 3\,xy, \end{cases} \tag{2.11}$$

where $b > 0$.

Corollary 2.3. *When $\mu = 0$, a subcritical Hopf bifurcation occurs at the origin for system* (2.11)*, which generates one unstable limit cycle when μ is negative but not too small. For $\mu = 0$, the origin is unstable.*

Proof. Note that $b > 0$ and system (2.11) is a special case of (2.5) with $c = 1$.

By setting $c = 1$ in (2.10), we have

$$a_1 = \frac{23\,b^2 + 60b + 24}{80b\,(b^2 + 4)} > 0, \tag{2.12}$$

where a_1 is the first Lyapunov number. According to Proposition 2.2, conditions (2.6) and (2.7), and the sign of (2.12), we have the conclusions. □

The following results give us insights into the stability of the system (2.5).

Proposition 2.3. *Consider system* (2.5) *with $\mu \neq 0$ and $b > 0$. The stability properties of the origin are characterized as follows:*

(i) If $-2 < \mu < 0$, the origin is a stable node-focus.

(ii) If $0 < \mu < 2$, the origin is a saddle-focus of index 2.

(iii) If $\mu \leq -2$, the origin is a stable node.

(iv) If $\mu \geq 2$, the origin is a saddle of index 2.

Proof. The Jacobian matrix of the system at the origin is

$$A = \begin{bmatrix} 0 & 1 & 0 \\ -1 & \mu & 0 \\ 0 & 0 & -b \end{bmatrix}.$$

The corresponding characteristic polynomial is

$$\varphi_A(\lambda) = (\lambda + b)(\lambda^2 - \mu\,\lambda + 1). \tag{2.13}$$

By analyzing of the roots of (2.13), we can draw the four conclusions. □

2.3. Chameleon chaotic dynamics with μ varying

Consider the following three systems:

$$\begin{cases} \dfrac{dx}{dt} = y, \\ \dfrac{dy}{dt} = -x + y(z + \mu), \\ \dfrac{dz}{dt} = y^2 - 0.7\,x^2 - 3\,xy, \end{cases} \tag{2.14}$$

$$\begin{cases} \dfrac{dx}{dt} = y, \\ \dfrac{dy}{dt} = -x + y(z + \mu), \\ \dfrac{dz}{dt} = 0.001 + y^2 - 0.7\,x^2 - 3\,xy, \end{cases} \tag{2.15}$$

$$\begin{cases} \dfrac{dx}{dt} = y, \\ \dfrac{dy}{dt} = -x + y(z + \mu), \\ \dfrac{dz}{dt} = -0.01\,z + y^2 - 0.7\,x^2 - 3\,xy, \end{cases} \tag{2.16}$$

where $\mu \in [-0.08, 0.02]$. These systems can be obtained from system (2.1) by setting $(a, b, c) = (0, 0, 1)$, $(a, b, c) = (0.001, 0, 1)$, and $(a, b, c) = (0, 0.01, 1)$, respectively. Figure 1 shows the bifurcation diagrams for these systems with respect to the parameter μ.

Let $(L_1^{(k)}, L_2^{(k)}, L_3^{(k)})$, $k = 1, 2, 3$, be the Lyapunov exponent spectra of systems (2.14), (2.15), and (2.16), respectively. For each k, the exponents satisfy $L_1^{(k)} > 0$, $L_2^{(k)} = 0$, and $L_3^{(k)} < 0$. The variations of $L_1^{(k)}$ and $L_3^{(k)}$ with respect to the parameter μ for $1 \le k \le 3$ are shown in Figure 2.

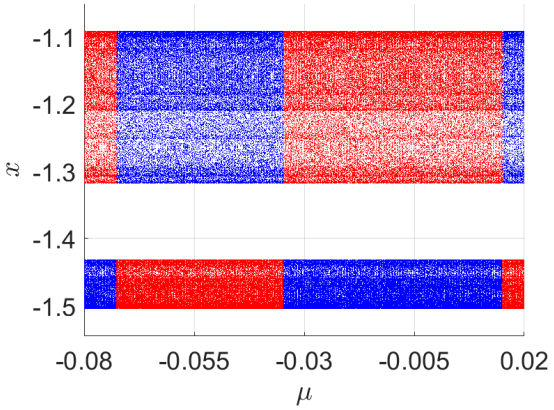

(a) System (2.14)

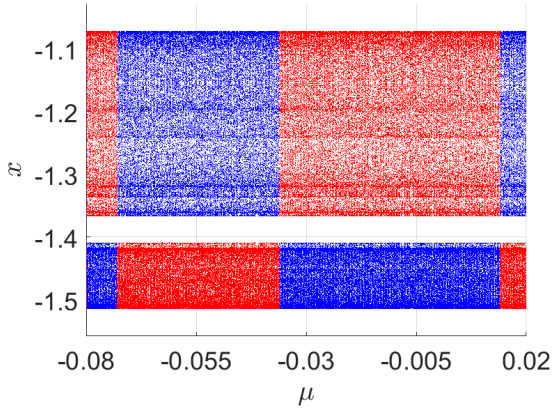

(b) System (2.15)

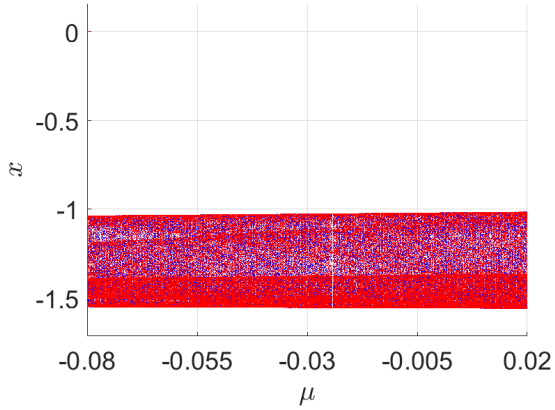

(c) System (2.16)

Figure 1. Bifurcation diagrams of systems (2.14)–(2.16) with respect to the parameter μ. Initial data: $(0.8, 0.8, 0)$ (blue), $(-0.8, -0.8, 0)$ (red).

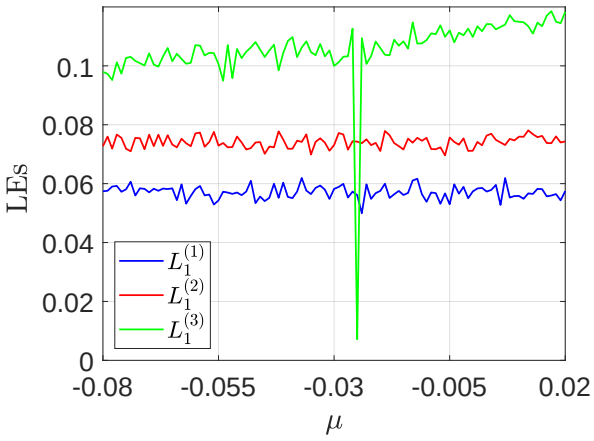

(a)

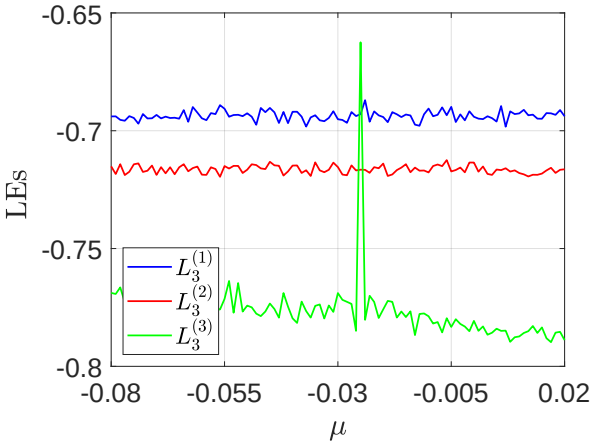

(b)

Figure 2. Lyapunov exponents of systems (2.14)–(2.16) with respect to the parameter μ. Initial conditions: $(0.8, 0.8, 0)$. (a) $L_1^{(k)}$, $k = 1, 2, 3$, (b) $L_3^{(k)}$, $k = 1, 2, 3$.

Based on the two figures above and the nature of equilibrium points, we classify the dynamical behaviors of these three systems into four scenarios:

Scenario 1: Hidden chaotic dynamics with a line equilibrium Note that system (2.14) has a line equilibrium $x = y = 0$. Thus, from panel (a) of Figure 1, we see that system (2.14) exhibits a symmetric pair of hidden chaotic attractors for $\mu \in [-0.08, 0.02]$, coexisting with a line equilibrium.

Scenario 2: Hidden chaotic dynamics without equilibrium It is clear that there is no equilibrium in system (2.15). Thus, from panel (b) of Figure 1, we see that system (2.15) exhibits a symmetric pair of hidden chaotic attractors without an equilibrium point for $\mu \in [-0.08, 0.02]$.

Scenario 3: Hidden chaotic dynamics with a stable equilibrium By Proposition 2.3, we know that system (2.16) has a stable equilibrium at the origin when $\mu \in [-0.08, 0)$. Thus, from panel (c) of Figure 1, we see that system (2.16) exhibits a symmetrical hidden chaotic attractor for $\mu \in [-0.08, 0)$.

Scenario 4: Self-excited chaotic dynamics with an unstable equilibrium By Corollary 2.3 and Proposition 2.3, we know that system (2.16) has an unstable equilibrium at the origin when $\mu \in [0, 0.02]$. Thus, from panel (c) of Figure 1, we see that system (2.16) exhibits a symmetrical self-excited chaotic attractor for $\mu \in [0, 0.02]$.

3. Bifurcation analysis for scenarios 1 to 4 with $\mu = 0$

Using two fixed initial conditions and varying parameters c and a, we demonstrate the system's period-doubling routes to chaos when $\mu = 0$. The analysis reveals that system (2.1) can exhibit either self-excited or hidden chaotic attractors under different parameter settings.

3.1. Scenario 1 with c varying: Hidden chaotic dynamics with a line equilibrium

Let

$$f_1(x, y) = y^2 - 0.7\,x^2 - 3\,xy, \tag{3.1}$$

$$f_2(x, y) = 1.008\,y^2 - 0.7\,x^2 - 3\,xy. \tag{3.2}$$

3.1.1. Coexistence of asymmetric hidden chaotic attractors

When $\mu = 0$ and $f(x, y, z) = f_1(x, y)$, system (2.1) becomes

$$\begin{cases} \dfrac{dx}{dt} = y, \\ \dfrac{dy}{dt} = -x + yz, \\ \dfrac{dz}{dt} = y^2 - 0.7\,x^2 - 3\,xy. \end{cases} \tag{3.3}$$

It has a symmetric pair of hidden chaotic attractors with a line equilibrium, which is shown in Figure 3 by initiating with $(x, y, z) = (\pm 0.8, \pm 0.8, 0)$. Figure 4 shows various projections of the coexisting hidden chaotic attractors. The corresponding Poincaré maps for the two attractors are shown in Figure 5. The set of dense points covering a certain region on the plane $y = 0$ shows that each attractor is chaotic. When the initial conditions are set to $(0.8, 0.8, 0)$, system (3.3) has Lyapunov exponents of $(L_1, L_2, L_3) = (0.0548, 0, -0.6914)$ and a Kaplan-Yorke dimension of $D_{\mathrm{KY}} = 2 - L_1/L_3 \approx 2.079$.

The sum of the three exponents $L_1 + L_2 + L_3 = -0.6366$ signifies that the system exhibits dissipative behavior, characterized by a chaotic attractor.

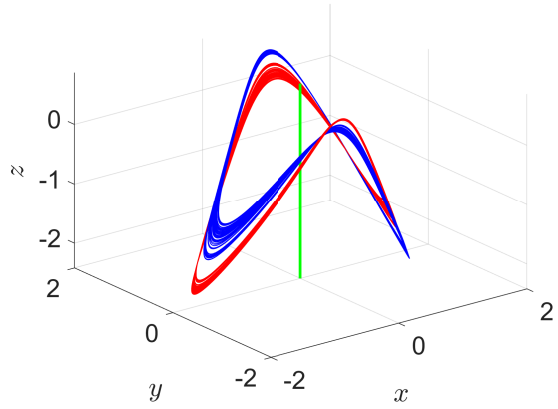

Figure 3. A symmetric pair of hidden chaotic attractors of system (3.3) with a line equilibrium (green). Initial data: $(-0.8, -0.8, 0)$ (red), $(0.8, 0.8, 0)$ (blue).

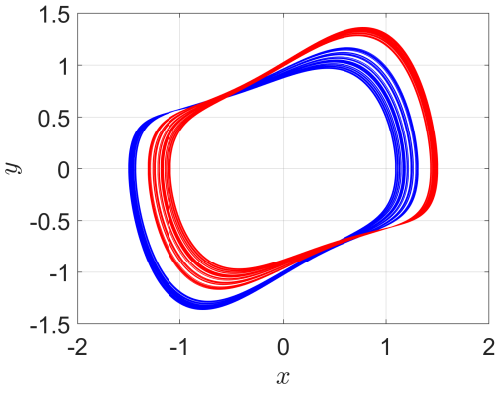

(a) x-y plane

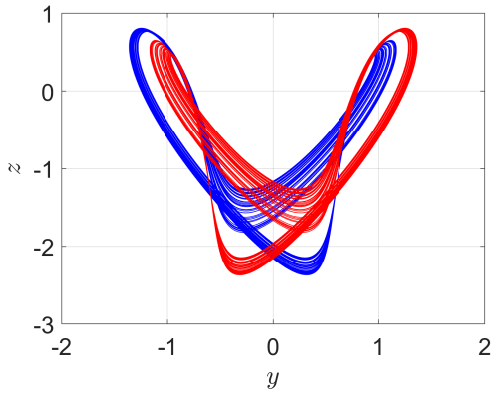

(b) y-z plane

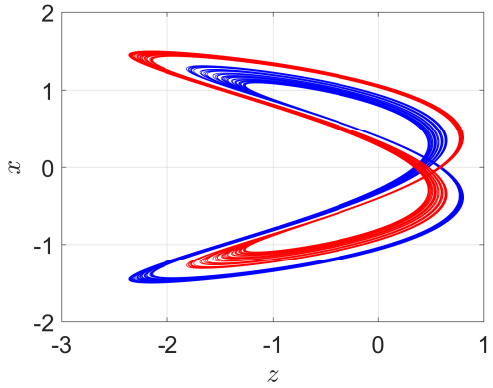

(c) z-x plane

Figure 4. Projections of coexisting hidden chaotic attractors of system (3.3). (a) x-y plane, (b) y-z plane, (c) z-x plane.

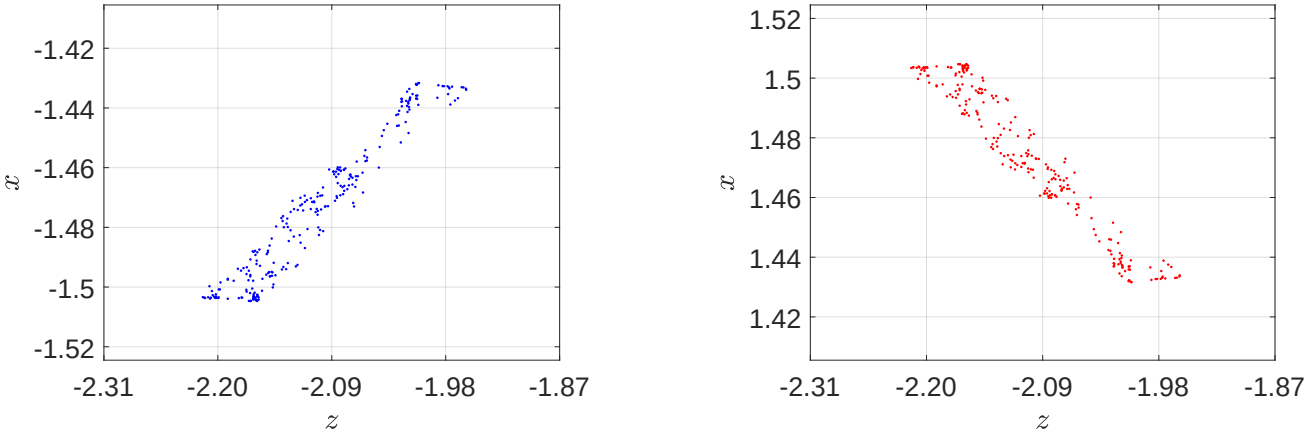

(a) **(b)**

Figure 5. Poincaré maps of system (3.3) on the plane $y = 0$. Initial conditions: $(\pm 0.8, \pm 0.8, 0)$. (a) For $(0.8, 0.8, 0)$ and $\frac{dy}{dt} > 0$. (b) For $(-0.8, -0.8, 0)$ and $\frac{dy}{dt} < 0$.

3.1.2. Symmetrical hidden chaotic attractor

When $\mu = 0$ and $f(x, y, z) = f_2(x, y)$, system (2.1) becomes

$$\begin{cases} \dfrac{dx}{dt} = y, \\ \dfrac{dy}{dt} = -x + yz, \\ \dfrac{dz}{dt} = 1.008\, y^2 - 0.7\, x^2 - 3\, xy. \end{cases} \tag{3.4}$$

It has a symmetric hidden chaotic attractor with respect to the z-axis, which is visualized in Figure 6 by starting from the initial conditions $(x, y, z) = (0.8, 0.8, 0)$. Moreover, the line equilibrium z-axis is denoted by a green line. The Poincaré maps of the attractor are shown in Figure 7, in which forward and backward directions are considered, respectively. When the initial conditions are set to $(0.8, 0.8, 0)$, system (3.4) has Lyapunov exponents of $(L_1, L_2, L_3) = (0.1179, 0, -0.7641)$ and a Kaplan-Yorke dimension of $D_{\mathrm{KY}} = 2 - L_1/L_3 \approx 2.154$.

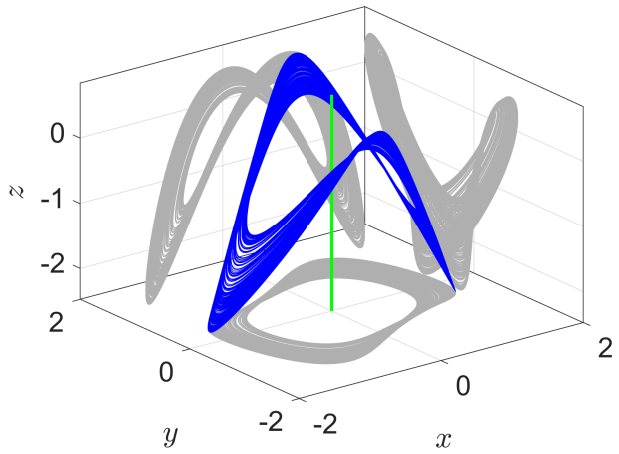

Figure 6. A symmetric hidden chaotic attractor of system (3.4) with a line equilibrium (green). Initial data: $(0.8, 0.8, 0)$ (blue).

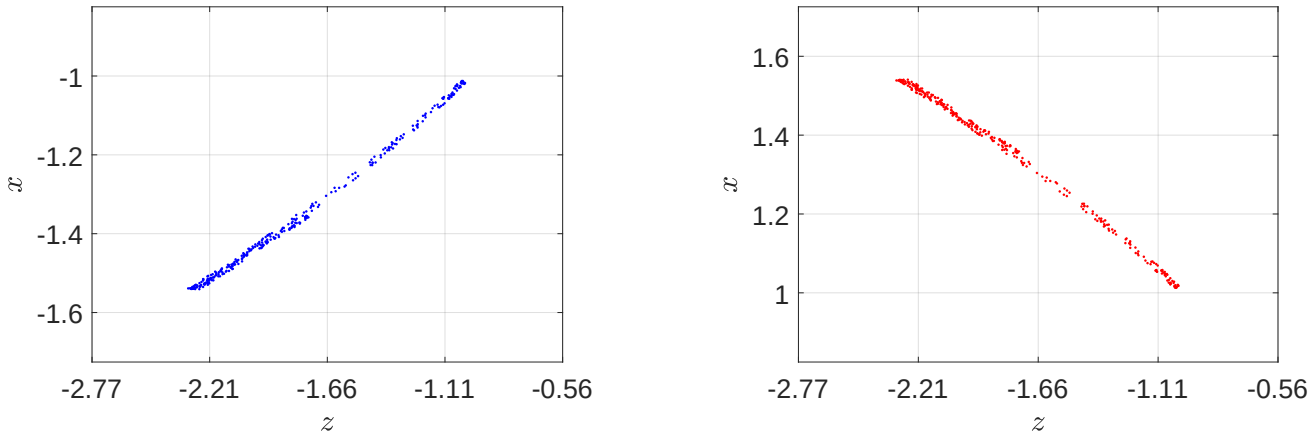

(a) **(b)**

Figure 7. Poincaré maps of system (3.4) on the plane $y = 0$. Initial conditions: $(0.8, 0.8, 0)$. (a) $\frac{dy}{dt} > 0$. (b) $\frac{dy}{dt} < 0$.

3.1.3. Bifurcation analysis

Consider the following system:

$$\begin{cases} \dfrac{dx}{dt} = y, \\ \dfrac{dy}{dt} = -x + yz, \\ \dfrac{dz}{dt} = c\,y^2 - 0.7\,x^2 - 3\,xy, \end{cases} \tag{3.5}$$

where $c \in [0.8, 1.008]$ is the coefficient of the nonlinear term y^2. It contains systems (3.3) and (3.4) as special cases.

For the two initial conditions $(\pm 0.8, \pm 0.8, 0)$, the bifurcation diagram is presented in Figure 8(a) for $c \in [0.94, 1.008]$. It shows the development of the hidden chaotic motions (with a line equilibrium) via period-doubling cascades. The periodic orbit undergoes a symmetry-breaking bifurcation around $c \approx 0.967$, transitioning into a saddle orbit, and giving rise to a pair of asymmetric stable periodic orbits. For each initial data, the first period-doubling bifurcation occurs at $c \approx 0.991$. The period and amplitude of the two asymmetric attractors grow with increasing c until they touch the saddle orbit and merge into a broader symmetrical hidden chaotic attractor at $c \approx 1.0027$ in an attractor merging crisis. Recall that an attractor merging crisis refers to two or more chaotic attractors merging to form a single attractor as the critical parameter value is passed [53]. For the initial data $(x(0), y(0), z(0)) = (0.8, 0.8, 0)$, the variations of Lyapunov exponents and their sum with respect to the parameter c are shown in Figure 8(b). The Lyapunov exponent spectrum depicted in Figure 8(b) aligns with the bifurcation diagram illustrated in Figure 8(a). In Figure 8(b), we also plotted the variation of $L_{\text{sum}} = L_1 + L_2 + L_3$ with respect to c. For each value of c, the sum L_{sum} is negative, indicating that the system is dissipative. Hence, the system is always dissipative for c within the interval $[0.94, 1.008]$.

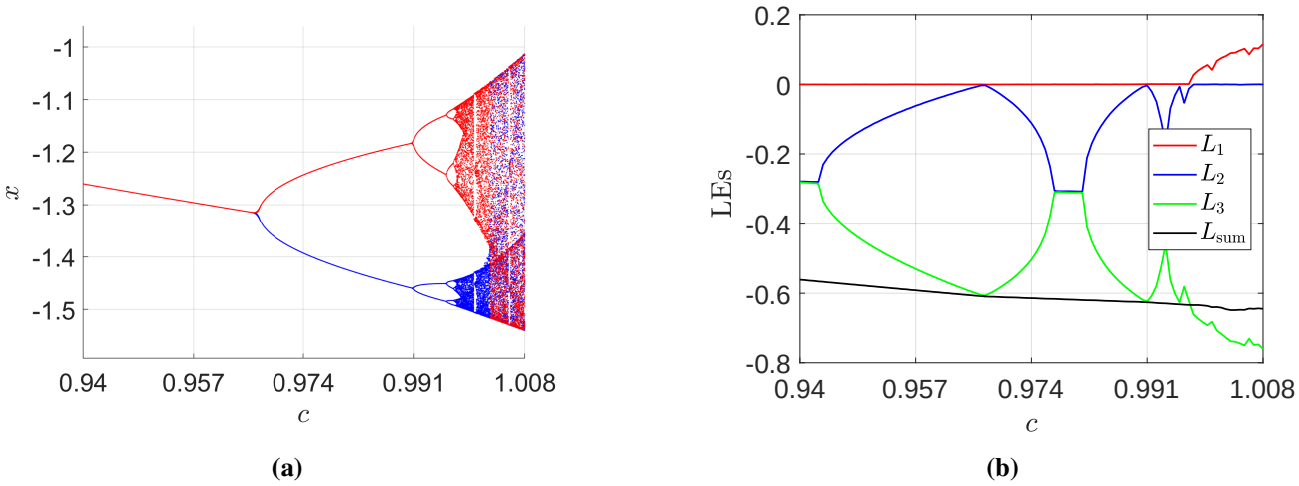

(a) **(b)**

Figure 8. Bifurcation diagram and Lyapunov exponent spectrum of system (3.5) with respect to c. (a) Initial data: $(0.8, 0.8, 0)$ (blue) and $(-0.8, -0.8, 0)$ (red), (b) Initial data: $(0.8, 0.8, 0)$.

3.2. Scenario 2 with a varying: Hidden chaotic dynamics without equilibrium

Letting $b = \mu = 0$ in system (2.1), we have the following system:

$$\begin{cases} \dfrac{dx}{dt} = y, \\ \dfrac{dy}{dt} = -x + yz, \\ \dfrac{dz}{dt} = a + (y^2 - 0.7\,x^2 - 3\,xy). \end{cases} \tag{3.6}$$

When $a \neq 0$, it has no equilibrium but does exhibit an invariant straight line along the z-axis. Recall that when $a = 0$, the system can have a symmetric pair of hidden chaotic attractors with a line equilibrium (z-axis).

For the two initial conditions $(\pm 0.8, \pm 0.8, 0)$, the bifurcation diagram is presented in Figure 9(a) for $a \in [-0.02, 0.004]$. It shows the development of the hidden chaotic motions (with no equilibrium) via period-doubling cascades. The left panel of Figure 9 with the change of a is qualitative similar to Figure 8(a) with the change of c. For the initial data $(x(0), y(0), z(0)) = (0.8, 0.8, 0)$, the variation of Lyapunov exponents with respect to the parameter a is shown in Figure 9(b). Note that at $a \approx 0.0013$, a symmetric pair of hidden chaotic attractors combine into a symmetrical hidden chaotic attractor. At $a = 0.004$, there exists a symmetrical hidden chaotic attractor with a Lyapunov exponent spectrum of $(L_1, L_2, L_3) = (0.1162, 0, -0.7621)$ and a Kaplan-Yorke dimension of 2.152.

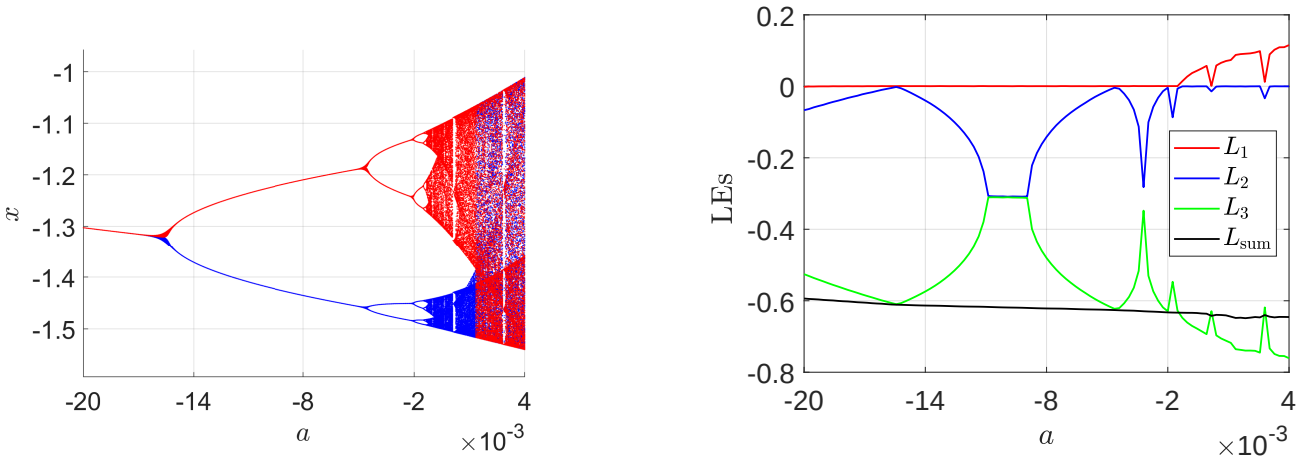

(a) **(b)**

Figure 9. Bifurcation diagram and Lyapunov exponent spectrum of system (3.6) with respect to a. (a) Initial data: $(0.8, 0.8, 0)$ (blue) and $(-0.8, -0.8, 0)$ (red), (b) Initial data: $(0.8, 0.8, 0)$.

3.3. Scenarios 3 and 4 with a varying: Hidden chaotic dynamics with a stable equilibrium and self-excited chaotic dynamics with an unstable equilibrium

Letting $b = 0.01, \mu = 0$ in system (2.1), we have the following system:

$$\begin{cases} \dfrac{dx}{dt} = y, \\ \dfrac{dy}{dt} = -x + yz, \\ \dfrac{dz}{dt} = (a - 0.01\,z) + (y^2 - 0.7\,x^2 - 3\,xy), \end{cases} \tag{3.7}$$

which has a single equilibrium at $P: \ (0, 0, 100a)$. According to Corollary 2.2, the equilibrium P is locally asymptotically stable for $a < 0$.

For the two initial conditions $(\pm 0.8, \pm 0.8, 0)$, the bifurcation diagram is presented in Figure 10(a) for $a \in [-0.03, 0]$. It shows the development of chaotic motions via period-doubling cascades. For the initial data $(x(0), y(0), z(0)) = (0.8, 0.8, 0)$, the variation of Lyapunov exponents with respect to the parameter a is show in Figure 10(b). From Figure 10, there is a narrow range near $a = 0$ with $a < 0$ that corresponds to hidden chaotic dynamics with a stable node-focus.

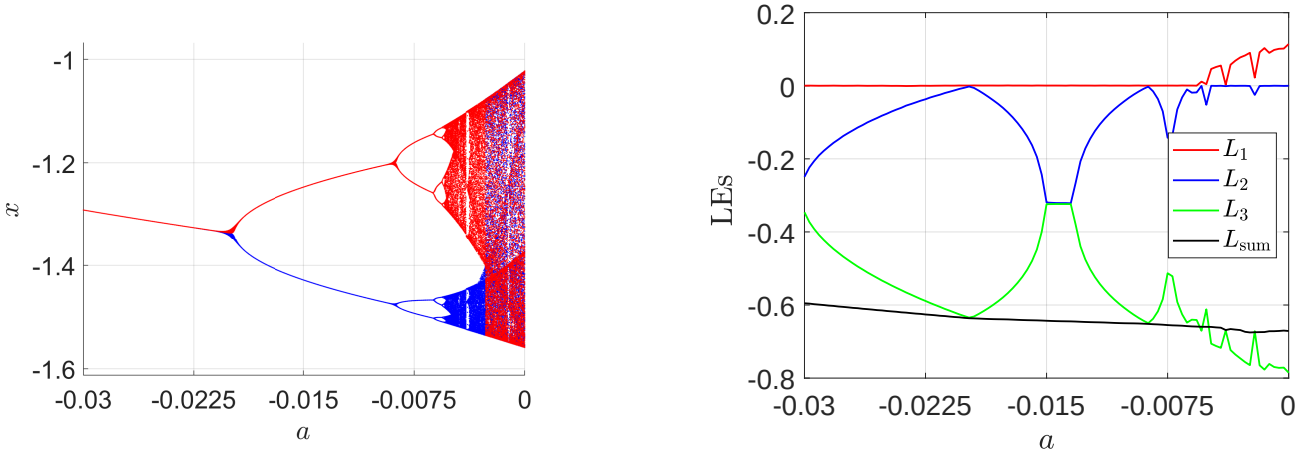

(a) **(b)**

Figure 10. Bifurcation diagram and Lyapunov exponent spectrum of system (3.7) with respect to a in the range $[-0.03, 0]$. (a) Initial data: $(0.8, 0.8, 0)$ (blue) and $(-0.8, -0.8, 0)$ (red), (b) Initial data: $(0.8, 0.8, 0)$.

For two initial conditions $(\pm 0.8, \pm 0.8, 0)$, the bifurcation diagram is presented in Figure 11 for $a \in [0, 2\times 10^{(-4)}]$. When $a = 0$, from (2.12), we know that the first Lyapunov number a_1 of system (3.7) is positive, thus the origin is unstable. Recalling from Corollary 2.2 that the equilibrium P is a saddle-focus of index 2 for $a \in (0, 2\times 10^{(-4)}]$, hence, we have that the chaotic range $[0, 2\times 10^{(-4)}]$ corresponds to self-excited dynamics.

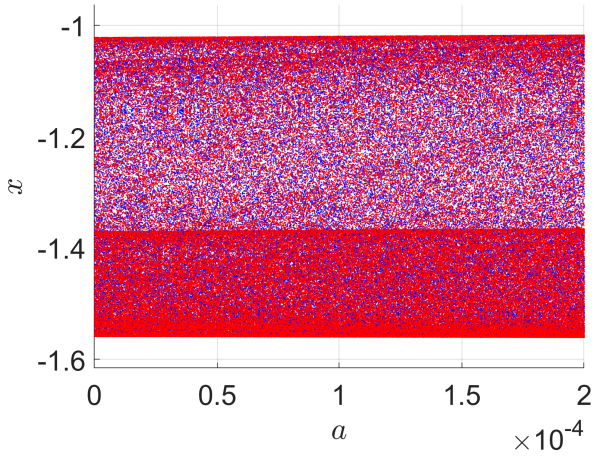

Figure 11. Bifurcation diagram of system (3.7) with respect to a in the range $[0, 2 \times 10^{(-4)}]$. Initial data: $(0.8, 0.8, 0)$ (blue), $(-0.8, -0.8, 0)$ (red).

4. Hidden chaotic bistability with offset boosting

With two initial conditions $(\mp 0.8, \mp 0.8, -\mu)$, the variations of the average values of the state variables in systems (2.14) and (2.15) with respect to μ are shown in Figures 12 and 13, respectively. Since the difference between the two system is caused by a small constant of 0.001, the figures are

almost the same. For both systems, the average value of z decreases smoothly as the parameter μ increases.

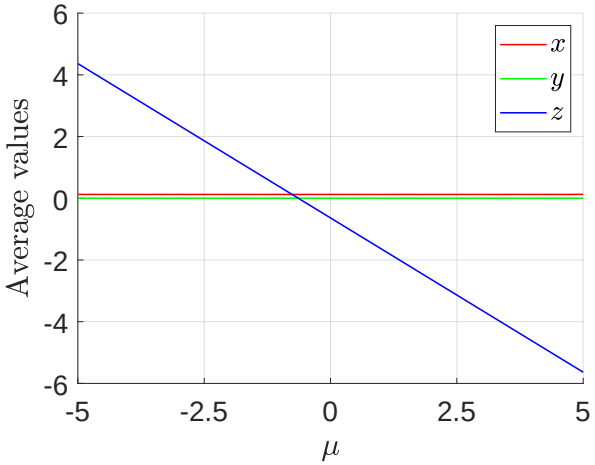

(a) Initial data: $(-0.8, -0.8, -\mu)$

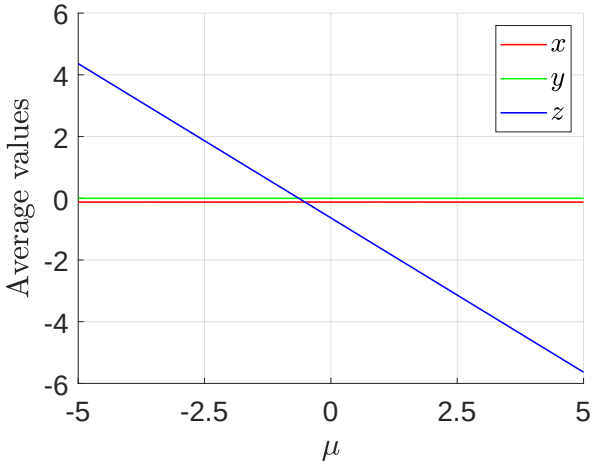

(b) Initial data: $(0.8, 0.8, -\mu)$

Figure 12. Variation of the average values of the state variables with respect to μ for different initial conditions in system (2.14). (a) Initial data: $(-0.8, -0.8, -\mu)$, (b) Initial data: $(0.8, 0.8, -\mu)$.

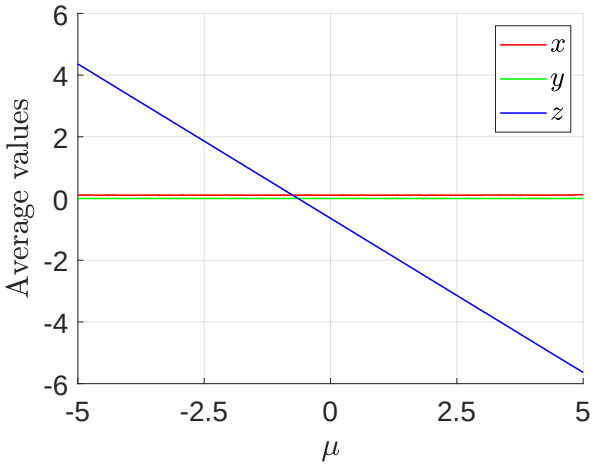

(a) Initial data: $(-0.8, -0.8, -\mu)$

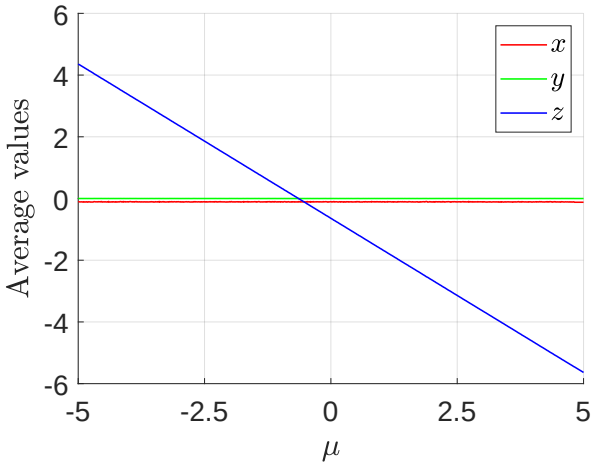

(b) Initial data: $(0.8, 0.8, -\mu)$

Figure 13. Variation of the average values of the state variables with respect to μ for different initial conditions in system (2.15). (a) Initial data: $(-0.8, -0.8, -\mu)$, (b) Initial data: $(0.8, 0.8, -\mu)$.

Let $(L_1^{(k)}, L_2^{(k)}, L_3^{(k)})$, $k = 1, 2$, be the Lyapunov exponent spectra of systems (2.14) and (2.15), respectively. For each k, we have $L_1^{(k)} > 0$, $L_2^{(k)} = 0$, and $L_3^{(k)} < 0$. For $1 \leq k \leq 2$, the variations of $L_1^{(k)}$ and $L_3^{(k)}$ with respect to the parameter μ are shown in Figure 14.

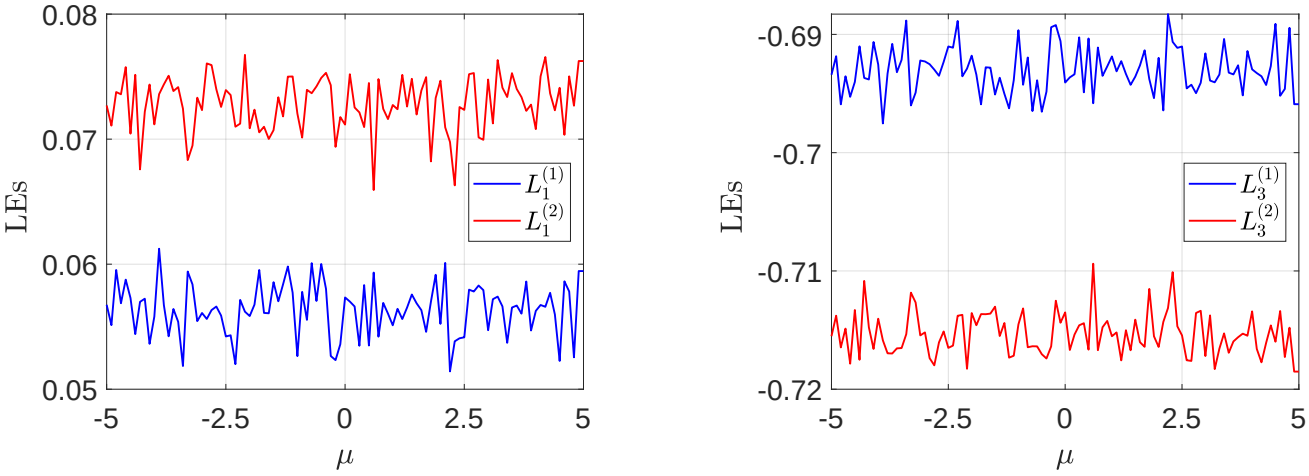

(a) **(b)**

Figure 14. Lyapunov exponents of systems (2.14) and (2.15) with respect to the parameter μ. Initial conditions: $(0.8, 0.8, -\mu)$. (a) $L_1^{(k)}$, $k = 1, 2$, (b) $L_3^{(k)}$, $k = 1, 2$.

Figure 14 indicates that as the initial conditions vary with the parameter μ, both of these systems exhibit chaotic dynamics. For system (2.14), there exists a symmetric pair of hidden chaotic attractors accompanied by an infinite number of equilibrium points. As for system (2.15), there also exists a symmetric pair of hidden chaotic attractors, but there are no equilibrium points. As shown in panel (a) of Figure 14, the largest Lyapunov exponent $L_1^{(2)}$ (red curve) of system (2.15) consistently exceeds the largest Lyapunov exponent $L_1^{(1)}$ (blue curve) of system (2.14), indicating that system (2.15) demonstrates stronger chaotic dynamics than system (2.14).

For systems (2.14) and (2.15) with $\mu = -5, 5$, the coexistence of hidden chaotic attractors is illustrated in Figures 15 and 16, respectively.

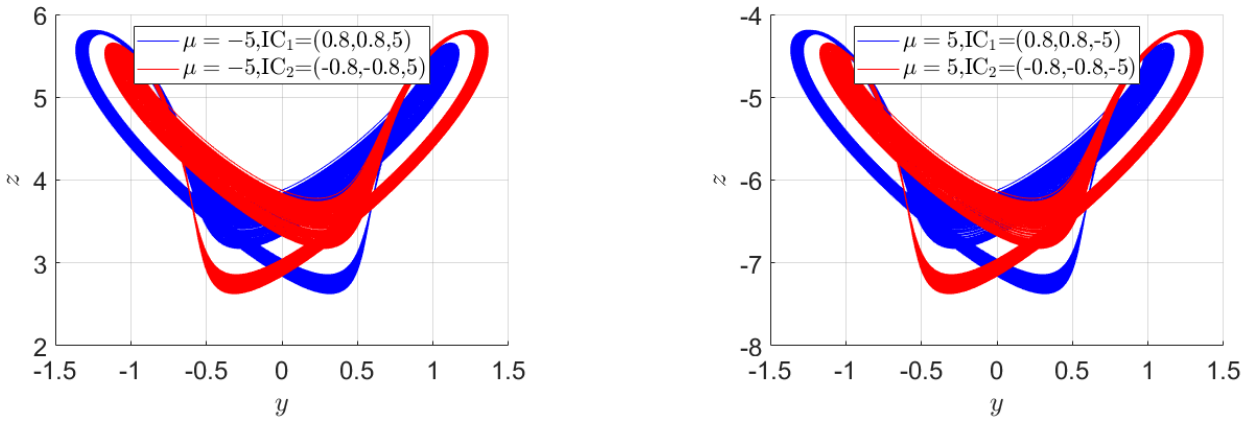

(a) $\mu = -5$ **(b)** $\mu = 5$

Figure 15. A symmetric pair of hidden chaotic attractors in system (2.14) for $\mu = -5$ and $\mu = 5$.

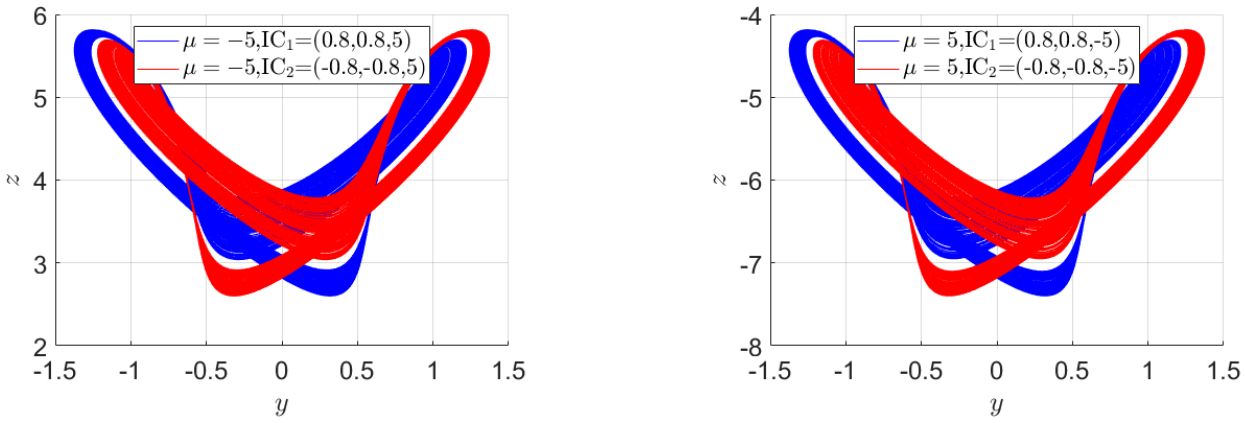

(a) $\mu = -5$ **(b)** $\mu = 5$

Figure 16. A symmetric pair of hidden chaotic attractors in system (2.15) for $\mu = -5$ and $\mu = 5$.

5. Conclusions

In this paper, we have conducted a comprehensive investigation of a novel chameleon system, examining its symmetry, dissipation, stability analysis, Hopf bifurcation, and various chaotic dynamics. The parameter μ serves as both the Hopf bifurcation parameter and the offset boosting parameter. The other parameters are also critical control parameters, with variation of which, the system undergoes period-doubling bifurcations leading to various types of chaos, including hidden chaos and self-excited chaos, with hidden chaos being predominant. By offset boosting the variable z, we also investigated the coexistence of hidden chaotic attractors. The results of this study enrich our understanding of the dynamical behavior of chameleon systems, providing important insights for research in related fields such as information security, cryptography, and nonlinear dynamics. In the future, it is hoped that there will be studies about chameleon systems subjected to small random perturbations.

Author contributions

Jie Liu: Writing-first draft. Bo Sang: Conceptualization, Writing-second and third drafts. Lihua Fan: Software. Chun Wang: Software. Xueqing Liu: Software. Ning Wang: Conceptualization, Software. Irfan Ahmad: Conceptualization. All authors have read and approved the final version of the manuscript for publication.

Use of Generative-AI tools declaration

The authors declare they have not used Artificial Intelligence (AI) tools in the creation of this article.

Acknowledgments

This research is supported by the Shandong Provincial Natural Science Foundation (No. ZR2018MA025).

Conflict of interest

The authors declare that they have no competing interests in this paper.

References

1. R. A. Meyers, *Encyclopedia of physical science and technology* , San Diego: Academic Press, 1992.
2. C. Li, W. Hu, J. C. Sprott, X. Wang, Multistability in symmetric chaotic systems, *Eur. Phys. J. Spec. Top.*, **224** (2015), 1493–1506. https://doi.org/10.1140/epjst/e2015-02475-x
3. T. A. Alexeeva, N. V. Kuznetsov, T. N. Mokaev, Study of irregular dynamics in an economic model: attractor localization and Lyapunov exponents, *Chaos Soliton. Fract.*, **152** (2021), 111365. https://doi.org/10.1016/j.chaos.2021.111365
4. S. Vaidyanathan, A. S. T. Kammogne, E. Tlelo-Cuautle, C. N. Talonang, B. Abd-El-Atty, A. A. Abd El-Latif, et al., A novel 3-D jerk system, its bifurcation analysis, electronic circuit design and a cryptographic application, *Electronics*, **12** (2023), 2818. https://doi.org/10.3390/electronics12132818
5. C. Nwachioma, J. H. P'erez-Cruz, Analysis of a new chaotic system, electronic realization and use in navigation of differential drive mobile robot, *Chaos Soliton. Fract.*, **144** (2021), 110684. https://doi.org/10.1016/j.chaos.2021.110684
6. N. V. Kuznetsov, G. A. Leonov, V. I. Vagaitsev, Analytical-numerical method for attractor localization of generalized Chua's system, *IFAC Proc. Vol.*, **43** (2010), 29–33. https://doi.org/10.3182/20100826-3-TR-4016.00009
7. G. A. Leonov, N. V. Kuznetsov, V. I. Vagaitsev, Localization of hidden Chua's attractors, *Phys. Lett. A*, **375** (2011), 2230–2233. https://doi.org/10.1016/j.physleta.2011.04.037
8. G. A. Leonov, N. V. Kuznetsov, Hidden attractors in dynamical systems. From hidden oscillations in Hilbert-Kolmogorov, Aizerman, and Kalman problems to hidden chaotic attractor in Chua circuits, *Int. J. Bifurcat. Chaos*, **23** (2013), 1330002. https://dx.doi.org/10.1142/S0218127413300024
9. N. V. Stankevich, N. V. Kuznetsov, G. A. Leonov, L. O. Chua, Scenario of the birth of hidden attractors in the Chua circuit, *Int. J. Bifurcat. Chaos*, **27** (2017), 1730038. https://doi.org/10.1142/S0218127417300385
10. N. Kuznetsov, T. Mokaev, V. Ponomarenko, E. Seleznev, N. Stankevich, L. Chua, Hidden attractors in Chua circuit: mathematical theory meets physical experiments, *Nonlinear Dyn.*, **111** (2023), 5859–5887. https://doi.org/10.1007/s11071-022-08078-y

11. Q. Wu, Q. Hong, X. Liu, X. Wang, Z. Zeng, A novel amplitude control method for constructing nested hidden multi-butterfly and multiscroll chaotic attractors, *Chaos Soliton. Fract.*, **134** (2020), 109727. https://doi.org/10.1016/j.chaos.2020.109727
12. H. Tian, Z. Wang, P. Zhang, M. Chen, Y. Wang, Dynamic analysis and robust control of a chaotic system with hidden attractor, *Complexity*, **2021** (2021), 8865522. https://doi.org/10.1155/2021/8865522
13. F. Bao, S. Yu, How to generate chaos from switching system: a saddle focus of index 1 and heteroclinic loop-based approach, *Math. Probl. Eng.*, **2011** (2011), 756462. https://doi.org/10.1155/2011/756462
14. T. Zhou, G. Chen, Classification of chaos in 3-D autonomous quadratic systems-I: basic framework and methods, *Int. J. Bifurcat. Chaos*, **16** (2006), 2459–2479. https://doi.org/10.1142/S0218127406016203
15. Z. Wei, J. C. Sprott, H. Chen, Elementary quadratic chaotic flows with a single non-hyperbolic equilibrium, *Phys. Lett. A*, **379** (2015), 2184–2187. https://doi.org/10.1016/j.physleta.2015.06.040
16. K. Rajagopal, V. T. Pham, F. R. Tahir, A. Akgul, H. R. Abdolmohammadi, S. Jafari, A chaotic jerk system with non-hyperbolic equilibrium: dynamics, effect of time delay and circuit realisation, *Pramana*, **90** (2018), 52. https://doi.org/10.1007/s12043-018-1545-x
17. X. Cai, L. Liu, Y. Wang, C. Liu, A 3D chaotic system with piece-wise lines shape non-hyperbolic equilibria and its predefined-time control, *Chaos Soliton. Fract.*, **146** (2021), 110904. https://doi.org/10.1016/j.chaos.2021.110904
18. C. Li, W. Hai, Constructing multiwing attractors from a robust chaotic system with non-hyperbolic equilibrium points, *Automatika*, **59** (2018), 184–193. https://doi.org/10.1080/00051144.2018.1516273
19. C. Li, J. C. Sprott, Chaotic flows with a single nonquadratic term, *Phys. Lett. A*, **378** (2014), 178–183. https://doi.org/10.1016/j.physleta.2013.11.004
20. S. Jafari, J. C. Sprott, F. Nazarimehr, Recent new examples of hidden attractors, *Eur. Phys. J. Spec. Top.*, **224** (2015), 1469–1476. https://doi.org/10.1140/epjst/e2015-02472-1
21. X. Wang, G. Chen, A chaotic system with only one stable equilibrium, *Commun. Nonlinear Sci.*, **17** (2012), 1264–1272. https://doi.org/10.1016/j.cnsns.2011.07.017
22. X. Wang, A. Akgul, S. Cicek, V. T. Pham, D. V. Hoang, A chaotic system with two stable equilibrium points: dynamics, circuit realization and communication application, *Int. J. Bifurcat. Chaos*, **27** (2017), 1750130. https://doi.org/10.1142/S0218127417501309
23. P. C. Rech, Self-excited and hidden attractors in a multistable jerk system, *Chaos Soliton. Fract.*, **164** (2022), 112614. https://doi.org/10.1016/j.chaos.2022.112614
24. V. T. Pham, S. Jafari, C. Volos, T. Kapitaniak, A gallery of chaotic systems with an infinite number of equilibrium points, *Chaos Soliton. Fract.*, **93** (2016), 58–63. https://doi.org/10.1016/j.chaos.2016.10.002
25. M. Molaie, S. Jafari, J. C. Sprott, S. M. Golpayegani, Simple chaotic flows with one stable equilibrium, *Int. J. Bifurcat. Chaos*, **23** (2013), 1350188. https://doi.org/10.1142/S0218127413501885

26. S. Jafari, J. C. Sprott, Simple chaotic flows with a line equilibrium, *Chaos Soliton. Fract.*, **57** (2013), 79–84. https://doi.org/10.1016/j.chaos.2013.08.018

27. S. Kumarasamy, M. Banerjee, V. Varshney, M. D. Shrimali, N. V. Kuznetsov, A. Prasad, Saddle-node bifurcation of periodic orbit route to hidden attractors, *Phys. Rev. E*, **107** (2023), L052201. https://doi.org/10.1103/PhysRevE.107.L052201

28. R. Balamurali, J. Kengne, R. G. Chengui, K. Rajagopal, Coupled van der Pol and Duffing oscillators: emergence of antimonotonicity and coexisting multiple self-excited and hidden oscillations, *Eur. Phys. J. Plus*, **137** (2022), 789. https://doi.org/10.1140/epjp/s13360-022-03000-2

29. B. Li, B. Sang, M. Liu, X. Hu, X. Zhang, N. Wang, Some jerk systems with hidden chaotic dynamics, *Int. J. Bifurcat. Chaos*, **33** (2023), 2350069. https://doi.org/10.1142/S0218127423500694

30. C. Dong, M. Yang, L. Jia, Z. Li, Dynamics investigation and chaos-based application of a novel no-equilibrium system with coexisting hidden attractors, *Phys. A*, **633** (2024), 129391. https://doi.org/10.1016/j.physa.2023.129391

31. J. C. Sprott, Strange attractors with various equilibrium types, *Eur. Phys. J. Spec. Top.*, **224** (2015), 1409–1419. https://doi.org/10.1140/epjst/e2015-02469-8

32. M. A. Jafari, E. Mliki, A. Akgul, V. T. Pham, S. T. Kingni, X. Wang, S. Jafari, Chameleon: the most hidden chaotic flow, *Nonlinear Dyn.*, **88** (2017), 2303–2317. https://doi.org/10.1007/s11071-017-3378-4

33. K. Rajagopal, A. Karthikeyan, P. Duraisamy, Hyperchaotic chameleon: fractional order FPGA implementation, *Complexity*, **2017** (2017), 8979408. https://doi.org/10.1155/2017/8979408

34. H. Natiq, M. R. Said, M. R. Ariffin, S. He, L. Rondoni, S. Banerjee, Self-excited and hidden attractors in a novel chaotic system with complicated multistability, *Eur. Phys. J. Plus*, **133** (2018), 557. https://doi.org/10.1140/epjp/i2018-12360-y

35. S. Cang, Y. Li, R. Zhang, Z. Wang, Hidden and self-excited coexisting attractors in a Lorenz-like system with two equilibrium points, *Nonlinear Dyn.*, **95** (2019), 381–390. https://doi.org/10.1007/s11071-018-4570-x

36. Q. Yang, Z. Wei, G. Chen, An unusual 3D autonomous quadratic chaotic system with two stable node-foci, *Int. J. Bifurcat. Chaos*, **20** (2010), 1061–1083. https://doi.org/10.1142/S0218127410026320

37. V. F. Signing, G. G. Tegue, M. Kountchou, Z. T. Njitacke, N. Tsafack, J. D. Nkapkop, et al., A cryptosystem based on a chameleon chaotic system and dynamic DNA coding, *Chaos Soliton. Fract.*, **155** (2022), 111777. https://doi.org/10.1016/j.chaos.2021.111777

38. W. Fan, D. Xu, Z. Chen, N. Wang, Q. Xu, On two-parameter bifurcation and analog circuit implementation of a chameleon chaotic system, *Phys. Scr.*, **99** (2023), 015218. https://doi.org/10.1088/1402-4896/ad1231

39. A. Tiwari, R. Nathasarma, B. K. Roy, A new time-reversible 3D chaotic system with coexisting dissipative and conservative behaviors and its active non-linear control, *J. Franklin I.*, **361** (2024), 106637. https://doi.org/10.1016/j.jfranklin.2024.01.038

40. R. Zhou, Y. Gu, J. Cui, G. Ren, S. Yu, Nonlinear dynamic analysis of supercritical and subcritical Hopf bifurcations in gas foil bearing-rotor systems, *Nonlinear Dyn.*, **103** (2021), 2241–2256. https://doi.org/10.1007/s11071-021-06234-4

41. N. V. Stankevich, N. V. Kuznetsov, G. A. Leonov, L. O. Chua, Scenario of the birth of hidden attractors in the Chua circuit, *Int. J. Bifurcat. Chaos*, **27** (2017), 1730038. https://doi.org/10.1142/S0218127417300385

42. H. Zhao, Y. Lin, Y. Dai, Hopf bifurcation and hidden attractor of a modified Chua's equation, *Nonlinear Dyn.*, **90** (2017), 2013–2021. https://doi.org/10.1007/s11071-017-3777-6

43. M. Liu, B. Sang, N. Wang, I. Ahmad, Chaotic dynamics by some quadratic jerk systems, *Axioms*, **10** (2021), 227. https://doi.org/10.3390/axioms10030227

44. Q. Yang, D. Zhu, L. Yang, A new 7D hyperchaotic system with five positive Lyapunov exponents coined, *Int. J. Bifurcat. Chaos*, **28** (2018), 1850057. https://doi.org/10.1142/S0218127418500578

45. Z. Li, K. Chen, Neuromorphic behaviors in a neuron circuit based on current-controlled Chua Corsage Memristor, *Chaos Soliton. Fract.*, **175** (2023), 114017. https://doi.org/10.1016/j.chaos.2023.114017

46. Y. Liu, Y. Zhou, B. Guo, Hopf bifurcation, periodic solutions, and control of a new 4D hyperchaotic system, *Mathematics*, **11** (2023), 2699. https://doi.org/10.3390/math11122699

47. C. Li, J. C. Sprott, Variable-boostable chaotic flows, *Optik*, **127** (2016), 10389–10398. https://doi.org/10.1016/j.ijleo.2016.08.046

48. C. Li, A. Akgul, L. Bi, Y. Xu, C. Zhang, A chaotic jerk oscillator with interlocked offset boosting, *Eur. Phys. J. Plus*, **139** (2024), 242. https://doi.org/10.1140/epjp/s13360-024-05040-2

49. C. Li, X. Wang, G. Chen, Diagnosing multistability by offset boosting, *Nonlinear Dyn.*, **90** (2017), 1335–1341. https://doi.org/10.1007/s11071-017-3729-1

50. X. Gao, Hamilton energy of a complex chaotic system and offset boosting, *Phys. Scr.*, **99** (2024), 015244. https://doi.org/10.1088/1402-4896/ad1739

51. X. Zhang, C. Li, T. Lei, H. Fu, Z. Liu, Offset boosting in a memristive hyperchaotic system, *Phys. Scr.*, **99** (2024), 015247. https://doi.org/10.1088/1402-4896/ad156e

52. H. Dang-Vu, C. Delcarte, *Bifurcations et Chaos: une introduction à la dynamique contemporaine avec des programmes en Pascal, Fortran et Mathematica*, Paris: Ellipses, 2000.

53. C. Grebogi, E. Ott, J. A. Yorke, Chaos, strange attractors, and fractal basin boundaries in nonlinear dynamics, *Science*, **238** (1987), 632–638. https://doi.org/10.1126/science.238.4827.632